International Journal of Engineering Studies.
ISSN 0975-6469 Volume 10, Number 1 (2018), pp. 11–21

http://www.ripublication.com/ijes.htm

Optimization of two Schottky Diode Topology Mixer for Satellite Signal Reception by Substrate Selection

Dr Tarik Baldawi and Dr Ashraf Abuelhaija

Electrical Engineering Department,
Applied Science Private University,
Amman, Jordan.
Orcid ID: 0000-0001-7315-9088; Orcid ID : 0000-0002-6645-3833

Abstract

The objective of this work is to examine and compare mixers using Schottky diodes of different substrates that will optimize its performance for satellite signal reception. Mixers of two different kinds of mount were investigated. The analysis required the adoption of theoretical model used for calculation of parameters and performance. Measurements were made to compare the results. It was found that the type of mount is an important parameter affecting the performance and selection of mixers for such purposes.

AMS subject classification: 05C78.
Keywords: Schottky diode, Mixers, Satellite reception.

1. Introduction

Television reception via satellite is becoming wide-spread all over world. Mixers (frequency converters) are one of the essential part in the reception system of signal from satellite, and their choice is related to frequency band desired. The internal topology of the mixer is also important. Thus discussion was presented here for reasoning the choice of frequency range for operation and testing, and also on the mixer topology selected for the work presented in this paper. The aim of this work is to explore the characteristics of the mixer and the dependence of its operation on the substrate or mount being used in the internal topology of the circuit. Thus, a review of theoretical work executed previously was made and was exploited for the analysis of the model representing the mixer topology. Two mixer types with different substrate or diode mount were examined. The

mixers use Schottky diodes. Theoretical models were used to analyze the mixer circuit. The Schottky diode model was used to obtain the diode parameters using large signal nonlinear analysis. Then, these were used for small-signal linear analysis of the mixer circuit. The two diode mixer model was adopted to analyze the mixer with two different substrates. Measurements were carried out to obtain certain important characteristics and compared with the theoretical results. On comparison of the theoretical and measured results, it was shown that mixer performance is strongly related to the substrate being used as well as to the type of circuit arrangement [1, 2, 3, 4].

2. Reasoning the frequency range and mixer topology selected

The choice of frequency at which a satellite operates is determined by two main factors. The frequency must be chosen to avoid harmful interference and minimize the cost of transmission, or maximize its information carrying rate. Most of today's communication satellites carry enough transponders to utilize 500 MHz bandwidth. The 4/6 GHz band, was exclusively by commercial geosynchronous satellites during their first decade of operation. When the 4 GHz down link is used there is a limit imposed on the radiated satellite power to prevent interference with terrestrial common carrier systems.

Government and military satellites in many countries use the 7/8 GHz band, with 7.9 to 8.4 GHz up and 7.25 to 7.75 GHz down. Satellites are now being designed for 12/14 GHz band, using 14 to 14.5 GHz up and either 11.7 to 12.2 GHz down, or 10.95 to 11.2 and 11.45 to 11.7 down. Thus it is apparent now why the research work presented in this paper will be confined to the present trend of the art, that is, the 10 to 12 GHz range. Whether nonlinear (diode) or switching element (such as a Field Effect Transistor FET) is used, mixers can be divided into several classes: single ended, single balanced and double balanced. Single ended mixer is simple and has the lowest conversion loss. However, it suffers from sensitivity to terminations, no spurious response suppression , minimal tolerance to large signals and narrow bandwidth due to spacing between RF filter and mixer diode. The single balanced structure, using two diodes, tends to exhibit slightly higher conversion loss than single ended structure. Since RF signal is divided between two diodes then the signal power handling ability is better. However, more diodes require more LO power. The structure is balanced and therefore some isolation between ports is obtained and there is some spurious suppression for RF or LO products depending on which is balanced.

The double balanced structure, consists of diode bridge, exhibits the best large signal handling capability, port–to–port isolation, and spurious rejection. However it exhibits the poorest conversion loss and requires large LO drive. This has its area of application. There are topologies which employ multiple–rings with several diodes per leg to achieve the ultimate in large signal performance but require hundreds of mW of pump power. Having decided on the range of frequency and reviewed mixer topologies, the best choice is to use the two diode mixer topology. The mixers employed for the investigation will be examined for two types of substrate.

3. Mixer theory and model

A mixer, which can consist of any device capable of exhibiting nonlinear performance, is essentially a multiplier. That is, if at least two signals are present their product will be produced at the output. Figure (1) shows this concept. Unfortunately, no physical nonlinear device is perfect multiplier and the resulting output have sidebands ω_n thus

$$\omega_n = \omega_o \pm \omega_p \tag{3.1}$$

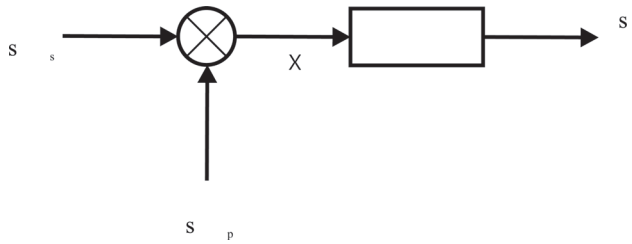

Figure 1:

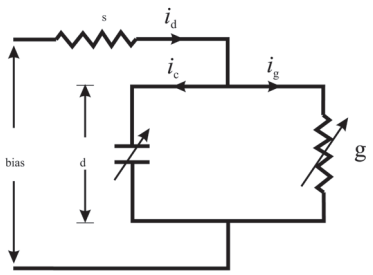

Figure 2:

The simple metal–semiconductor (Schottky barrier diodes) exhibits a nonlinear impedance as a function of the applied voltage and can be used in mixer design. This subject was dealt with extensively in literature. The diode model shown in Figure (2) was adopted for analysis in this work. In the model employed it was assumed that the diode conductance current ID obeys the thermionic emission:

$$I_D = I_s \left[exp\left(V_d/nV_T\right) - 1\right] \tag{3.2}$$

Where I_s is the reverse saturation current, V_T the thermal voltage and n is the diode ideality factor. This leads to:

$$\text{conductance, } g = \frac{I_D}{nV_T} \tag{3.3}$$

$$V_T = \frac{kT}{q} \approx 26\,\text{mV, thermal voltage} \tag{3.4}$$

$$C_j = \frac{C_{jo}}{(1 + \frac{V_R}{V_o})^m} \tag{3.5}$$

where C_{jo} is the value of C_j for zero applied voltage, V_R is the reverse applied voltage, V_o is the barrier voltage, and m is a constant whose value depends on the manner in which the concentration changes from p to n side of the junction, it is called the grading coefficient and its value ranges from 1/3 to 1/2. [5, 6]

In noise analysis the mixer diode model is modified as shown in Figure (3) to include shot noise due to current flow across the depletion layer, and also the thermal noise from the series resistance R_s.

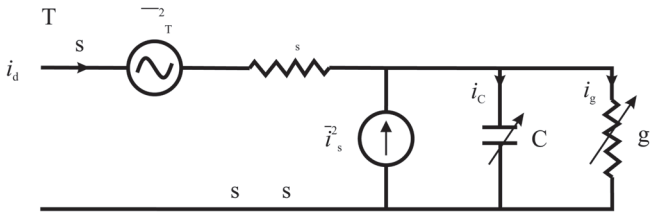

Figure 3:

Analytical work was carried out for mixer with single diode, two-diodes and any number of diodes. Since the objective of this work is to examine the suitability and properties of two-diodes mixer with different mount circuit, the two-diodes model shown in Figure (4) will be used.

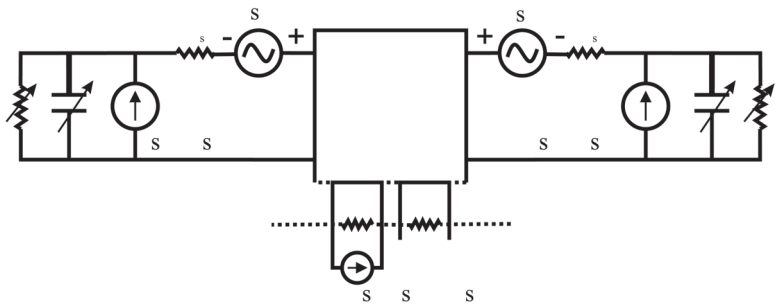

Figure 4:

The mixer was represented by a multi-frequency multiport network, shown in Figure (5), to represent the sidebands of the LO effect on various components. The model consisting of embedding network which contains the series resistance RS of the diodes and all source and load admittance Y_k connected externally to the diode mount. In normal mixer operation the ports shown in the model are all either open-circuited or connected to current sources at appropriate sideband frequencies. The ports numbering (x, k) is such that $x = (A, B \text{ or } D)$ indicating one of three sides of the embedding network, and

k indicates sideband frequency $\omega_k = \omega_p + k \cdot \omega_o$, where ω_o is the IF and ω_p is the LO frequency.

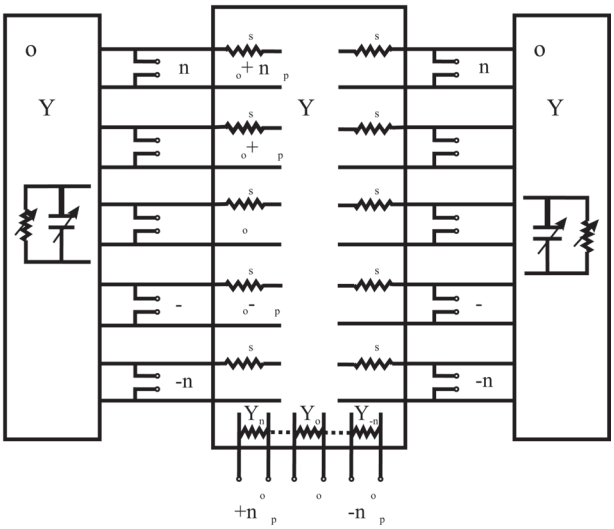

Figure 5:

4. Mixer Analysis

The analysis of the two diode mixer will be summarized as follows. The single Schottky diode model is used to obtain the diode parameters which will be used in the analysis of a single diode mixer. After completion of the analysis we proceed to the model representing the two diode mixer topology from which the final properties can be calculated.

4.1. Schottky diode model

Depending on the procedure outlined in reference (2), and using the large-signal Schottky diode model, the diode parameters envolved in the analysis of the mixer can be obtained easily. Thus the aim of this step is to enable us to carry out the large-signal nonlinear analysis on the diode.

4.2. Pumped diode mixer model

If LO power at ω_p is applied to a diode in a mixer then a large signal current and voltage waveform will be produced at the diode by the LO. The steady-state large signal response of a pumped diode can be described in terms of Fourier coefficient of V_d and i_d. Thus

$$V_d(t) = \sum_{k=-\infty}^{+\infty} V_k \cdot exp(jk\omega_p t), (V_k) = (V_{-k}^*) \tag{4.1}$$

$$i_d(t) = \sum_{k=-\infty}^{+\infty} I_d \cdot exp(jk\omega_p t), (I_d)_k = (I_d^*)_{-k} \tag{4.2}$$

The resulting periodic conductance and capacitance waveforms will be in general contain components at all harmonics ofω_p. Thus the small signal admittance components can be written as:

$$g(t) = \sum_{k=-\infty}^{+\infty} G_k \cdot exp(jk\omega_p t), (G_k) = (G_{-k}^*) \tag{4.3}$$

$$c(t) = \sum_{k=-\infty}^{+\infty} C_k \cdot exp(jk\omega_p t), (C_k) = (C_{-k}^*) \tag{4.4}$$

The waveforms $g(t)$ and $c(t)$ can be determined by computer program. The coefficient G_k and C_k and diode mount govern the small-signal properties of the mixer. The output sidebands will be $\omega_n = \omega_o \pm m\omega_p$. The resulting small-signal components of the diode voltage and current at sideband ω_m enables us to express the conversion properties of the diode as:

$$[\delta I] = [Y] \cdot [\delta V] \tag{4.5}$$

Is a square conversion admittance matrix of the intrinsic diode for a particular conductance and capacitance waveforms. The numbering of all matrices and vectors will correspond with sideband numbering given by:

$$Y_{mn} = G_{mn} + j\omega C_{mn} \tag{4.6}$$

Y is the admittance matrix of the intrinsic diode, but if the diode is mounted onto a circuit with impedance $Z_{\omega m}$ then a new augmented matrix $\left[Y^M\right]$ results. The new matrix expresses the network including all sideband embedding impedances

$$\left[Y^M\right] = [Y] + dig\left[\frac{1}{Z_{\omega m}}\right] \tag{4.7}$$

4.3. Two diode mixer

Equations (4.6) and (4.7) allow the single diode matrix to be characterized for small-signal analysis as a multi-frequency multiport network with one port for each sideband frequency. This is demonstrated in Figure (5) and (6), for two pumped diodes (A and B) mixer connected via their mount to external sources and loads at various sideband frequencies ω_k. Thus the elements of the resulting conversion matrix will as below:

$$Y^{A/B} = G_{m-n}^{A/B} + j\omega C_{m-n}^{A/B} \tag{4.8}$$

Side D of the model is allocated for all source and load admittances Y_k connected externally to the diode mount. Thus the embedding network matrix can be written in portioned manner as:

$$\left[Y^E\right] = \begin{bmatrix} Y^E_{AA} & Y^E_{AB} & Y^E_{AD} \\ Y^E_{BA} & Y^E_{BB} & Y^E_{BD} \\ Y^E_{DA} & Y^E_{DB} & Y^E_{DD} \end{bmatrix} \tag{4.9}$$

It is assumed that the embedding network is linear and no internal coupling between ports at different sideband frequencies and hence the only nonzero elements are those for which $m = n$. The sub-matrices are all diagonal matrices, e.g.:

$$\left[Y^E_{AA}\right] = \begin{bmatrix} Y^E_{(A,n)(A,n)} & Y^E_{(A,n)(A,1)} & Y^E_{(A,n)(A,0)} & Y^E_{(A,n)(A,-n)} \\ Y^E_{(A,1)(A,n)} & Y^E_{(A,1)(A,1)} & Y^E_{(A,1)(A,0)} & Y^E_{(A,1)(A,-n)} \\ Y^E_{(A,0)(A,n)} & Y^E_{(A,0)(A,1)} & Y^E_{(A,0)(A,0)} & Y^E_{(A,0)(A,-n)} \\ Y^E_{(A,-1)(A,n)} & Y^E_{(A,-1)(A,1)} & Y^E_{(A,-1)(A,0)} & Y^E_{(A,-1)(A,-n)} \\ Y^E_{(A,-n)(A,n)} & Y^E_{(A,-n)(A,-1)} & Y^E_{(A,-n)(A,-1)} & Y^E_{(A,-n)(A,-n)} \end{bmatrix} \tag{4.10}$$

Where n represents sideband number of port which also correspond to the numbering of row or column in the matrix. The parallel connection of the two pumped diodes A and B with the $\left[Y^C\right]$ leads to the overall mixer admittance matrix given below as:

$$\left[Y^M\right] = \begin{bmatrix} Y^A + Y^E_{AA} & Y^C_{AB} & Y^C_{AD} \\ Y^C_{BA} & Y^C + Y^C_{BB} & Y^C_{BD} \\ Y^C_{DA} & Y^C_{DB} & Y^C_{DD} \end{bmatrix} \tag{4.11}$$

4.4. Analytical and Practical Measurements

Using the V-I diode relationship, the Schottky diode equivalent circuit and equations (3.1) to (3.5) the diode parameters could be obtained easily at room temperature. Two computer programs were then used. The first program is used for large- signal nonlinear analysis to obtain the Capacitance C and the conductance G. The second program is used for matrices conversion and calculating the mixer characteristics: input impedance Z_{in}, output impedance Z_{out}, noise figure NF and the conversion loss LO. To limit the size of the matrices, the sidebands were limited to four only.

If the load admittance Y_{Load} is considered as equal to zero at IF port $(D, 0)$, then the admittance matrix of the mixer becomes $Y^{M/OC}$ and the impedance seen there will be as follows:

$$\left[Z^{M/OC}\right] \approx \left[Y^M\right]^{-1} \tag{4.12}$$

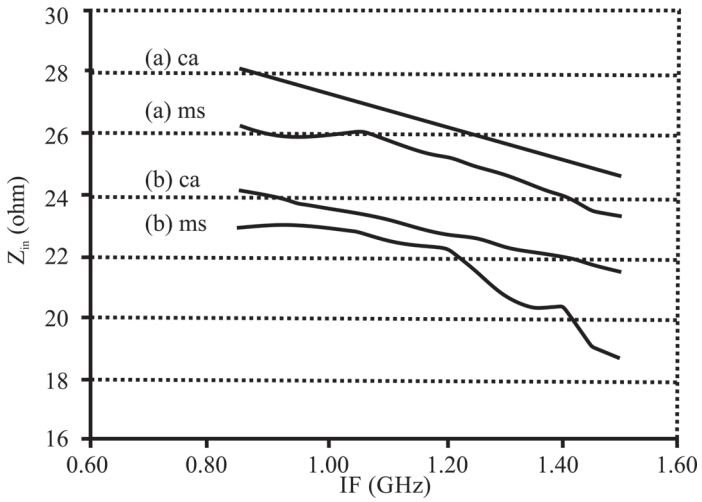

Figure 6: Variation of Z_{in} with frequency

Where $\left[Y^M\right]$is the modification of $\left[Y^E\right]$. Thus the output impedance of the mixer is given by matrix element $(D,0)(D,0)$ of $Z^{M/OC}$, so

$$Z_{out} = Z^{M/OC}_{(D,0)(D,0)} \tag{4.13}$$

For optimum conversion loss, the output terminal of the mixer should be the conjugate matched, only if

$$Y_0 = \left[1/Z_{(D,0)(D,0)}\right]^* \tag{4.14}$$

Inverting the mixer admittance matrix gives the impedance matrix:

$$\left[Z^M\right] \approx \left[Y^M\right]^{-1} \tag{4.15}$$

The conversion loss between any side-bands ω_k and the IF port $(D,0)$ is defined as the ratio of the power available from source to power delivered to the load. Assuming optimum conversion loss conditions and diodes A and B are similar (current sharping), then:

$$\text{Loss at mid band} = \frac{1}{4 \mid Z^M_{(D,0)(D,0)} \mid^2 \cdot Re\left[Y_k\right] \cdot Re\left[Y_o\right]} \tag{4.16}$$

The impedance $Z_{port}(D,k)$ at any sideband is given by the appropriate element of $\left[Z^M\right]$:

$$Z_{port}(D,k) = Z^M(D,k) \tag{4.17}$$

This impedance results from paralleling the source admittance Y_k and the mixer itself. Thus the input impedance of the mixer is the impedance seen by the admittance and it is

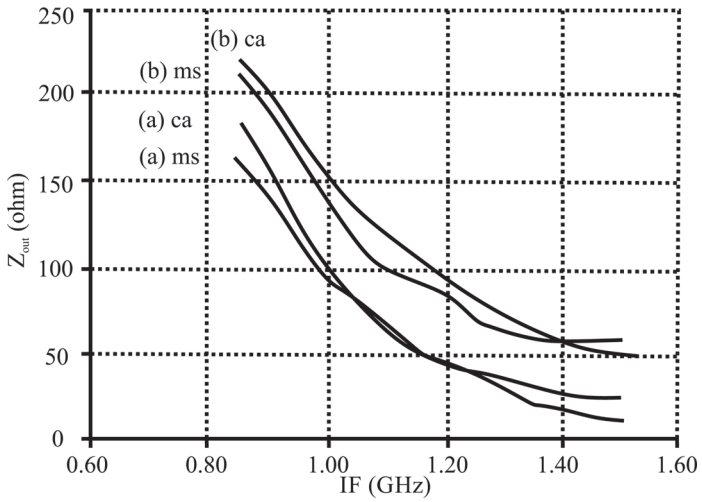

Figure 7: Variation of Z_{out} with frequency

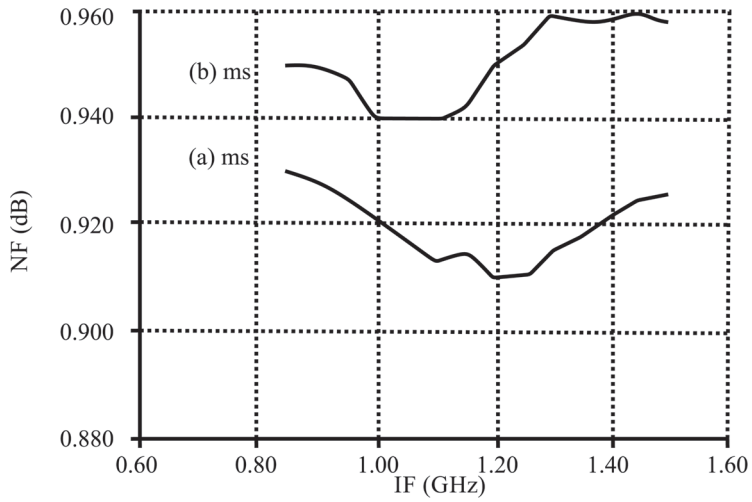

Figure 8: Noise figure with frequency

the matrix element:

$$Z_{in\ k} = \left[\frac{1}{Z^{M}_{(D,k)(D,k)}} - Y_k \right] \tag{4.18}$$

For practical measurements hybrid integrated mixers were made available facilitating the use of the same Schottky diodes. The mixer performance was examined for two types of substrates. The LO frequency driving the mixer was operated between 9–11 GHz for the range of IF to be tested. The same measuring procedure and setup were followed for both types of mixers.

5. Results and Discussion

Measured (ms) and calculated (ca) results of various mixer characteristics were plotted against the output terminal frequency IF. Figure (6) shows the comparative results between measured and calculated input impedance Zin of the mixers with two diode topology having Alumine (a) and DUROID (b) substrates. Figure (7) shows similar curves for the output impedance Z_{out}, while figure (8) shows the Noise Figure (NF) in db, which was not calculated but measured only. The conversion loss has been calculated only. Caiculation was made with LO frequency of 10.75 GHz for RF input signal of 12.1 GHz, corresponding to the upper sideband, and for 0.95 GHz , corresponding to the lower sideband. The calculated conversion loss, for the upper sideband, was 4.2 dB for mixer (a) and 6.15 dB for mixer (b). These figures are not constant and change with frequency, but the result is quite informative. On comparing results, it was found that mixer (b) exhibit same behavior but tend to be of higher noise and conversion lost than that of mixer (a). The behavior and levels of various characteristics are well within the acceptable values normally specified for mixers operating at such frequency. The deviation of calculated results from those obtained by measurements could be due to errors from the practical measurements and also, probably, due to displacement of some matrix elements during matrix conversion.

6. Conclusion

Mixer performance for satellite signal reception and processing at 10–12 GHz can be optimized in two ways. Mixer optimization achieved by either selecting diode parameters for particular circuit substrate or optimization by selecting circuit substrate for a particular diodes. It was shown, in this work, that performance optimization of the mixer with two Schottky diodes topology depends on substrate selection for the mixer circuit.

Acknowledgement

This work has been done at the Applied Science Private University, Amman, JORDAN, Faculty of Engineering, department of Electrical Engineering. The authors would like to thank this university for their strong support to this work.

References

[1] K. L. Fong and R. G. Meyer, "Monolithic rf active mixer design," *IEEE Transactions on Circuits and Systems II: Analog and Digital Signal Processing*, vol. 46, no. 3, pp. 231–239.

[2] K. N. P. Usha, S. Vinushree, "Design and simulation of rf active mixer for c- band satellite transponder," *Int. Journal of Research and Scientific Innovation*, vol. IV, 2017.

[3] T. K. Johansen, J. Vidkjær, and V. Krozer, "Analysis and design of wide-band sige hbt active mixers," *IEEE transactions on microwave theory and techniques*, vol. 53, no. 7, pp. 2389–2397, 2005.

[4] C. Florian, F. Scappaviva, M. Feudale, V. Monaco, and F. Filicori, "AV band singly balanced diode mixer for space application," in *Gallium Arsenide and Other Semiconductor Application Symposium, 2005. EGAAS 2005. European*. IEEE, 2005, pp. 441–444.

[5] A. S. Sedra and K. C. Smith, *Microelectronic circuits*. New York: Oxford University Press, 2016.

[6] A. Sharma, P. Kumar, B. Singh, S. R. Chaudhuri, and S. Ghosh, "Capacitance-voltage characteristics of organic schottky diode with and without deep traps," *Applied Physics Letters*, vol. 99, no. 2, p. 130, 2011.